Spann, U., Renna, W., Mandelkow, E.-M., Bordas, J., & Mandelkow, E. (1987) *Biochemistry 26*, 1123–1132.
Tamm, L. K., Crepeau, R. H., & Edelstein, S. J. (1979) *J. Mol. Biol. 130*, 473–493.
Vallee, R. B., & Borisy, G. G. (1978) *J. Biol. Chem. 253*, 2834–2845.
Wang, J. L., & Edelman, G. M. (1971) *J. Biol. Chem. 246*, 1185–1191.
White, E. A., Burton, P. R., & Himes, R. H. (1987) *Cell Motil. Cytoskel. 7*, 31–38.
Williams, R. C., & Detrich, H. W. (1979) *Biochemistry 18*, 2499–2503.

Molecular Basis of the Heat Denaturation of Photosystem II†

Lynmarie K. Thompson, Richard Blaylock, Julian M. Sturtevant, and Gary W. Brudvig*
Department of Chemistry, Yale University, New Haven, Connecticut 06511
Received December 19, 1988; Revised Manuscript Received April 27, 1989

ABSTRACT: The thermal denaturation of the photosystem II (PSII) membrane protein complex is investigated by assigning the endothermic transitions observed by differential scanning calorimetry (DSC) to the denaturation of particular proteins of the PSII complex. In a prior DSC study of PSII membranes [Thompson, L. K., Sturtevant, J. M., & Brudvig, G. W. (1986) *Biochemistry 25*, 6161], five DSC peaks were observed in the 30–70 °C temperature range (A_1, A_2, B, C, and D). The A_2 peak was assigned to denaturation of a component essential for water oxidation and the B peak to denaturation of a component critical to the remainder of the electron-transport chain. We have now extended these studies with thermal gel analysis and electron paramagnetic resonance (EPR) measurements. Thermal gel analysis, a technique which relies on a change in the solubility properties of a membrane protein upon denaturation, has been used to determine the temperatures of denaturation of all of the major membrane proteins of the PSII complex. EPR experiments have been used to monitor chlorophyll photooxidation and the stability of Tyr_{D^+}. Peaks B, C, and D in the DSC denaturation profile are each assigned to the denaturaation of several proteins, which provides information on the organization of the PSII complex into structural and functional units. Peak B corresponds to the denaturation of peripheral core proteins and closely associated antenna proteins, peak C to the PSII core, and peak D to the loosely associated antenna proteins. No membrane protein is observed to denature during the A_2 peak. The A_2 peak is altered by the presence of catalase, superoxide dismutase, low chloride, and high pH. These results suggest that the abnormally sharp A_2 peak occurs when the highly oxidizing, sequestered Mn complex (the active site in water oxidation) becomes accessible to the aqueous phase, at elevated temperatures. We propose a mechanism for the reaction of the Mn complex with hydroxide ions, which involves peroxide or superoxide and results in the reduction and release of Mn. The proposed model provides insight into the well-known instability of the Mn complex and the role of chloride in stabilizing the complex. This may enable the future development of purification procedures and may explain the sensitivity of the water-oxidizing apparatus of PSII to heat denaturation.

Photosystem II (PSII)[1] is a multicomponent membrane protein complex which utilizes light energy to drive uphill electron-transport reactions and oxidize water. The water oxidation reaction, which occurs at an active site composed of four Mn ions, is the most heat-sensitive component of the entire photosynthetic electron-transport chain (Katoh & San Pietro, 1967). We have used differential scanning calorimetry (DSC) in combination with other techniques to investigate the heat denaturation of PSII, in order to provide insight into the structural organization of the complex and the individual roles of the component proteins, as well as to determine the molecular basis of the heat sensitivity of the water-oxidizing apparatus.

PSII utilizes a photon of light absorbed by P680, the special Chl primary electron donor, to catalyze electron transfer from water to plastoquinone:

$$H_2O \rightarrow \text{Mn complex} \rightarrow Tyr_Z \rightarrow P680 \rightarrow \text{pheophytin} \rightarrow Q_A \rightarrow Q_B$$

Components prior to P680 in this main electron-transfer chain

†This work was supported by the National Institutes of Health (GM32715) and the Herman Frasch Foundation. G.W.B. is the recipient of a Camille and Henry Dreyfus Teacher/Scholar award and an Alfred P. Sloan Foundation research fellowship. L.K.T. is the recipient of a dissertation fellowship from the American Association of University Women.

[1] Abbreviations: Chl, chlorophyll; DCBQ, 2,5-dichloro-*p*-benzoquinone; DCIP, 2,6-dichlorophenolindophenol; DCMU, 3-(3,4-dichlorophenyl)-1,1-dimethylurea; DPC, *sym*-diphenylcarbazide; DSC, differential scanning calorimetry; EPR, electron paramagnetic resonance; HEPES, *N*-(2-hydroxyethyl)piperazine-*N*′-2-ethanesulfonic acid; kDa, kilodalton(s); LHCP, light-harvesting chlorophyll *a*/*b* protein(s); MES, 2-(*N*-morpholino)ethanesulfonic acid; OGP, octyl glucopyranoside; PSII, photosystem II; P680, primary electron donor in PSII; Q_A, primary quinone electron acceptor in PSII (bound plastoquinone); Q_B, secondary quinone electron acceptor in PSII (plastoquinone binding site); SDS–PAGE, sodium dodecyl sulfate–polyacrylamide gel electrophoresis; Tris, tris(hydroxymethyl)aminomethane; Tyr_D, a Tyr residue which upon photooxidation gives rise to a dark-stable radical EPR signal; Tyr_Z, a Tyr residue which functions as the secondary electron donor in PSII; TX-100, Triton X-100.

0006-2960/89/0428-6686$01.50/0

Table I: Protein Composition of PSII Complexes

PSII	PSII core	LHCP	function
D1 (32 kDa)	D1 (32 kDa)		bind electron-transfer components: Tyr_Z, P680, pheophytin, Q_A, Q_B
D2 (34 kDa)	D2 (34 kDa)		
9 kDa	9 kDa		bind cytochrome b_{559} (two copies of each)
4 kDa	4 kDa		
47 kDa	47 kDa		bind chlorophyll
43 kDa	43 kDa		
29 kDa		29 kDa	
28 kDa	28 kDa		
22 kDa	22 kDa		?
10 kDa	10 kDa		?
LHCP (27 kDa)		27 kDa	LHCP: bind $\approx$ 150 antenna Chl
LHCP (25 kDa)		25 kDa	
33 kDa	33 kDa		extrinsic: stabilizes Mn binding
23 kDa	23 kDa		extrinsic: increase affinities for Ca^{2+} and Cl^- (cofactors in O_2 evolution)
17 kDa	17 kDa		

are known as the electron donor side; components beyond P680 are known as the electron acceptor side of PSII. Tyr_D, Chl, and cytochrome b_{559} are alternate electron donors (de Paula et al., 1985).

The roles of the many proteins of the PSII complex in the catalysis of electron transport and the structural organization of these proteins are not understood. PSII consists of about 12 membrane proteins and 3 extrinsic proteins, known by their approximate molecular weights and listed in Table I. The PSII complex can be separated into a core fraction, which contains the electron-transport chain and the water-oxidizing apparatus, and an antenna fraction, which coinsists of the light-harvesting Chl proteins (LHCP) and a 29-kDa Chl protein (Ikeuchi et al., 1985; Tang & Satoh, 1985; Ghanotakis & Yocum, 1986). The LHCP [25 and 27 kDa, about 15 copies per PSII, assuming 10 Chl/LHCP (Larsson & Andersson, 1985; Zuber, 1985)] bind about 150 antenna Chl which function to funnel light energy to the reaction center. The PSII core complex consists of proteins known as D1 and D2 (about 32 and 34 kDa), the cytochrome b_{559} proteins (9 and 4 kDa, two copies of each), a 22-kDa and a 10-kDa protein, three Chl proteins of 47, 43, and 28 kDa, and an extrinsic 33-kDa protein which stabilizes the Mn complex. Two other extrinsic proteins (17 and 23 kDa), which modulate the affinities for calcium and chloride (cofactors required for water oxidation), are present in some PSII core preparations. The simplest preparation of a PSII reaction center complex consists of D1, D2, and cytochrome b_{559}. This complex is unable to catalyze electron transport or water oxidation but can photoreduce the primary electron acceptor pheophytin (Nanba & Satoh, 1987). Recent analogies between PSII and the bacterial photosynthetic reaction center [see Michel and Deisenhofer (1988) and references cited therein] and studies of the electron donor side of PSII (Debus et al., 1988; Metz et al., 1986) suggest that this D1/D2/cytochrome b_{559} complex should bind most of the cofactors of PSII.

Although the location of the water-oxidizing apparatus in the PSII complex is unknown (indirect evidence suggests D1; Metz et al., 1986), the mechanism of the reaction and the composition of the active site are partially understood. The reaction consists of a catalytic cycle between five states, S_n, where $n = 0$–4 is the number of stored oxidizing equivalents. The sequential absorption of four photons advances the cycle from S_0 to S_4; O_2 is then rapidly released during $S_4 \rightarrow S_0$. The dark-stable state is S_1. This scheme was proposed to account for the observed periodicity of O_2 evolution, beginning on the third flash (Kok et al., 1970). The active site in the water oxidation reaction is now widely accepted to contain a complex of four Mn ions, which is thought to both bind water and store the oxidizing equivalents [reviewed by Brudvig et al. (1989)]. The heat denaturation of O_2 evolution has been shown to correlate with the release of two Mn ions (Cramer et al., 1981; Nash et al., 1985).

Our approach to the study of the heat denaturation of PSII has been first to use DSC to map out the denaturation profile of PSII. DSC scans of PSII samples (at pH 6.0, 0.01% TX-100) consist of at least five peaks: A_1 (47 °C), A_2 (48 °C), B (54 °C), C (60 °C), and D (66 °C) (Thompson et al., 1986). Each peak is an endothermic transition expected to correspond to the cooperative unfolding of one or more proteins. By assigning these peaks to the denaturation of individual proteins and activities of the PSII complex, one can obtain insight into the role of each protein as well as the association of these proteins into structures which each denature as independent cooperative units. Further insight into the denaturation reactions occurring during each DSC peak can be obtained by examining the effects of perturbing treatments on the DSC trace.

Heat inactivation studies have been used to assign the denaturation of two PSII activities to two of the DSC peaks. The denaturation of some component essential for water oxidation occurs during peak A_2, and the denaturation of some component critical to the remainder of the electron-transport chain occurs during peak B (Thompson et al., 1986). The assignment of the denaturation of O_2 evolution to a low-temperature shoulder in a DSC trace of thylakoid membranes was first made by Cramer et al. (1981). We have also shown that the A_2 peak is abnormally sharp, indicating an unusually cooperative denaturation, and have further investigated the nature of this denaturation by examining the effects of several treatments on this DSC peak. The oxidation state of cytochrome b_{559}, which has no effect on O_2 evolution activity, has a dramatic effect on the sharpness of the A_2 peak, suggesting that cytochrome b_{559} may play a structural role in the O_2-evolving complex (Thompson et al., 1986).

Thermal gel analysis, a technique which relies on the differential solubility of membrane proteins in the folded and unfolded states (Rigell et al., 1985), has been used to begin to assign the DSC peaks to the denaturations of four proteins of the PSII complex (Thompson et al., 1987). In this paper, we now extend these studies on PSII membrane, PSII core, and LHCP preparations and assign the denaturation of nearly all the proteins of the PSII complex to the peaks in the DSC trace. These results provide new insight into the structural associations among proteins within the PSII complex and demonstrate the utility of this approach for the study of structure and function in other large membrane protein complexes. We also examine the heat denaturation of some components and activities observable by EPR and investigate the effects of additional treatments on the A_2 peak in the DSC

trace. From these studies, we propose a mechanism for the molecular basis of the special heat sensitivity of the water-oxidizing apparatus.

Experimental Procedures

Sample Preparation. PSII membranes were isolated from spinach leaves by a modified version (Beck et al., 1985) of the method of Berthold et al. (1981). The PSII membranes to be used for heat denaturation studies were then washed via repeated resuspension and centrifugation to remove residual TX-100, which has been shown to alter the DSC denaturation profile, into either pH 6.0 buffer [20 mM MES–NaOH, pH 6.0, 15 mM NaCl, 5 mM $MgCl_2$, and 30% (v/v) ethylene glycol] or pH 7.5 buffer [20 mM HEPES–NaOH, pH 7.5, 15 mM NaCl, 5 mM $MgCl_2$, and 30% ethylene glycol (introduced as a cryoprotectant)] with 0.01% (w/v) TX-100 (Thompson et al., 1986). The PSII membrane samples exhibited O_2 evolution rates of 300–600 μmol of O_2 (mg of Chl)$^{-1}$ h^{-1}, with 250 μM DCBQ and 1 mM ferricyanide as electron acceptors. Chloride depletion of PSII membranes was performed by washing the sample twice in chloride depletion buffer (20 mM HEPES–NaOH, pH 7.5, 7.5 mM Na_2SO_4, 5 mM $MgSO_4$, and 30% ethylene glycol) plus 0.01% TX-100.

The PSII membranes were separated into the PSII core and LHCP fractions by the following procedure, based on that of Ghanotakis et al. (1987a). The PSII membranes were first transferred from 30% ethylene glycol into 0.4 M sucrose, by pelleting and resuspending 3 times in 0.4 M sucrose, 1% ethylene glycol, 10 mM NaCl, and 50 mM MES–NaOH, pH 6.0, at which point [ethylene glycol] = 1% (calculated by serial dilution). The final suspension was homogenized, adjusted to a concentration of 2.5 mg of Chl/mL, and then mixed with an equal volume of 70 mM OGP, 1 M sucrose, 0.8 M NaCl, 10 mM $CaCl_2$, and 50 mM MES–NaOH, pH 6.0. The sample was incubated 10 min and then diluted with 1 M sucrose, 0.4 M NaCl, 5 mM $CaCl_2$, and 50 mM MES–NaOH, pH 6.0, to reduce the [OGP] from 35 to 15 mM. After a 5-min incubation, this solution was centrifuged at 35000*g* for 20 min. The resulting supernatant is the PSII core fraction; the pellet is the LHCP fraction. The supernatant was desalted by two 30-min dialyses against 30% ethylene glycol, 10 mM NaCl, 5 mM $CaCl_2$, and 50 mM MES–NaOH, pH 6.0, until the sample was visibly aggregated, then diluted with an equal volume of the dialysis buffer, and centrifuged at 35000*g* for 30 min. The final pellet is the PSII core, and the supernatant is colorless. Both the PSII core and the LHCP fractions were washed 3 times into pH 7.5 buffer with 0.01% TX-100 for the DSC and thermal gel analysis experiments. The PSII core preparation activities were 1300–1500 μmol of O_2 (mg of Chl)$^{-1}$ h^{-1} in the presence of 10 mM $CaCl_2$, 250 μM DCBQ, and 1 mM ferricyanide. These sample manipulations were conducted at 4 °C in dim green light.

We found that the dilution step in the above procedure was critical for obtaining a good separation. If the [OGP] is diluted too much, both the LHCP and the PSII core will pellet; if it is diluted too little, neither will pellet. The difference between the optimum [OGP] we found and the procedure reported by Ghanotakis et al. (1987a) is probably due to a difference in the residual [TX-100].

Thermal Gel Analysis. For both thermal gel analysis studies of protein denaturation (Rigell et al., 1985) and EPR studies of heat inactivation, PSII samples identical with the DSC samples were heated in a water bath at the same heating rate as in the DSC experiment (1 °C/min) to the desired temperature and then placed on ice. The thermal gel analysis samples were then solubilized by adding pH 6.0 buffer and TX-100 from a 10% stock solution (in pH 6.0 buffer) to a final concentration of 5% TX-100 and 0.5 mg of Chl/mL. After a 20-min incubation, the solubilized samples were centrifuged 15 min at 35000*g*. The supernatants were prepared for SDS–PAGE on a 12.5% acrylamide gel with 5.5 M urea, according to the procedure of Chua et al. (1980). An alternate solubilization procedure was used in the thermal gel analysis study of cytochrome b_{559} and the 10-kDa proteins. The heated samples were first centrifuged 10 min at 35000*g*, and the pellets were then solubilized in 150 mM HEPES, pH 6.8, 4 M urea, and 2% TX-100 (Babcock et al., 1985). The SDS–PAGE was conducted on a 15% acrylamide gel.

The amount of each protein which can still be solubilized after the heat treatment was determined by measuring the peak height of the appropriate peaks in densitometry scans of each lane of the gels. For each protein, the relatively constant gel band intensities at low temperatures were averaged to determine a value corresponding to 100% solubilization, and the rapid decrease in intensity at high temperatures was fit to a line to determine the temperature of 50% solubilization, which is assumed to correspond to 50% denaturation ($T_{1/2}$).

Heat Inactivation. The samples were heated as described above and then assayed for either photoreduction of DCIP (30 μM), in the presence and absence of the artificial electron donor DPC (500 μM), or O_2 evolution activity [with 250 μM DCBQ and 1 mM $K_3Fe(CN)_6$ as artificial electron acceptors], in a buffer consisting of 25 mM MES–NaOH, pH 6.5, and 10 mM NaCl. The samples were prepared for EPR spectroscopy by the addition of 2.5 mM $K_3Fe(CN)_6$, followed by a 15-min incubation before freezing to 77 K. EPR spectra of the samples prior to illumination were used to measure the amount of dark-stable Tyr_{D^+}, by measuring the peak height of the low-field hyperfine line, which minimizes the interference from the Chl radical signal. The samples were then illuminated 10 min at 77 K. The relative intensity of the Chl cation radical in the illuminated-minus-dark difference spectra was determined by double integration of the EPR signal.

Differential Scanning Calorimetry (DSC). The DSC experiments were conducted in a DASM-4 (Figures 2 and 7) or a Microcal-2 (Figure 8) calorimeter, as previously described (Thompson et al., 1986). We assumed 230 Chl/PSII (equals 207-kDa Chl/995-kDa PSII) to compute the heat capacity scales of the figures. In Figure 2, the scale applies only to the DSC scan of PSII (Figure 2a); the core and LHCP scans were normalized to an equivalent number of PSII centers, so that the sum of these two scans (2b + 2c) is comparable to the PSII scan. For this normalization, we assumed 70 Chl/PSII core complex (Ghanotakis et al., 1987b). Because the Chl stoichiometry is not known for the impure LHCP preparation, we normalized scan 2b to obtain a roughly equivalent height for peak D in scans 2a and 2b (yielding a stoichiometry of 200 Chl/PSII in the LHCP preparation, which corresponds to the removal of about 50% of the core complex).

Results

Protein Denaturation Temperatures. (1) PSII Membranes. Thermal gel analysis can be used to determine the denaturation temperature of a protein which undergoes a change in solubility properties upon denaturation, as might be expected in particular of hydrophobic membrane proteins (Rigell et al., 1985). This technique utilizes gel electrophoresis to detemine the amount of each protein component which can be solubilized after heating a membrane protein suspension. In a prior thermal gel analysis study of PSII membrane samples (Thompson et al., 1987), we demonstrated that several PSII proteins behave as expected: when heated to temperatures

Table II: DSC Peak Assignments[a]

PSII membranes (pH 6.0)				
DSC peak	A_2 (47.5)	B (54.0)	C (59.5)	D (66.0)
protein denaturation	*b*	43 kDa (54)[c]	47 kDa (58)[c]	LHCP (63)[c]
		22 kDa (55)	29 kDa (59)	
			b_{559} (57)	
			10 kDa (57)	
PSII core fraction (pH 7.5)				
DSC peak	A_2 (33–38)	B (45–47)	C (53)	*d*
protein denaturation	*b*	43 kDa (43)	47 kDa (52)	*b*
		22 kDa (45)	D1 (52)	
		28 kDa (46)	D2 (51)	
LHCP fraction (pH 7.5)				
DSC peak	*d*	*d*	C (52.5)	D (66)
protein denaturation	*b*		47 kDa (51)	29 kDa (55)
				LHCP (56.57)

[a] Temperatures (degrees centigrade) are given in parentheses. [b] No protein denaturation observed. [c] These three protein denaturation assignments are from Thompson et al. (1987). [d] DSC peak not observed.

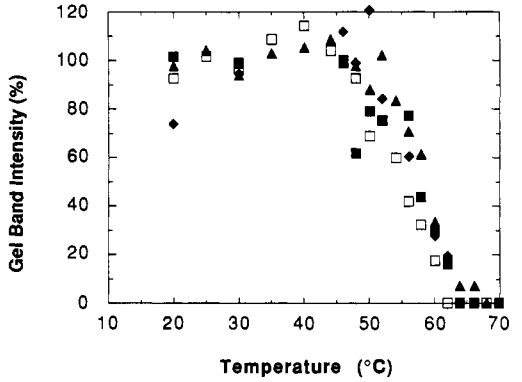

FIGURE 1: Thermal gel analysis of protein denaturation temperatures in a PSII preparation. Gel band intensities are plotted as a function of the temperature to which the aliquot was heated. The denaturation temperature ($T_{1/2}$) is assumed to be the temperature of 50% gel band intensity. The 29-kDa (▲, $T_{1/2}$ = 59 °C) and 22-kDa (□, $T_{1/2}$ = 55 °C) proteins were resolved on a 12.5% acrylamide gel; the 10-kDa (♦, $T_{1/2}$ = 57 °C) and the 9-kDa cytochrome b_{559} (■, $T_{1/2}$ = 57 °C) proteins were resolved on a 15% acrylamide gel. The denaturation of the proteins represented by open symbols correlates with peak B, and the closed symbols with peak C.

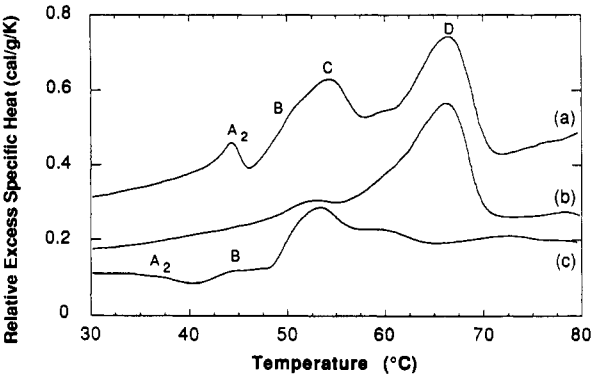

FIGURE 2: Comparison of the DSC behavior of PSII membranes with that of isolated PSII core and LHCP fractions. DSC scans of (a) PSII membranes, (b) LHCP, and (c) PSII core preparations, all in pH 7.5 buffer with 0.01% TX-100. The specific heat scale applies only to scan a, as discussed in the text.

below the denaturation temperature, there is no change in the amount of the protein which is solubilized, and thus the gel band intensity remains constant. At higher temperatures, the gel band intensity decreases sharply to zero, presumably due to a change in solubility upon denaturation. Thus, we determined the denaturation tempeatures given at the top of Table II for the two LHCP (which correlate with peak D), the 47-kDa protein (which correlates with peak C), and the 43-kDa protein (which correlates with peak B; Thompson et al., 1987).

Several other protein denaturation temperatures in PSII membrane samples are now assigned by using thermal gel analysis as shown in Figure 1. The 22-kDa protein denatures at 55 °C, which is assigned to peak B (54.0 °C), and the 29-kDa protein denatures at 59 °C, which is assigned to peak C (59.5 °C). In order to assign the denaturation temperature of the 9-kDa protein of cytochrome b_{559}, we utilized alternate solubilization conditions (Babcock et al., 1985) which were more effective in solubilizing this protein. A higher percent acrylamide gel was used to resolve the 9- and 10-kDa low molecular mass proteins. Both the 9- and 10-kDa proteins denature at 57 °C and are assigned to peak C. The 4-kDa cytochrome b_{559} protein probably denatures at the same temperature as the 9-kDa protein, and is thus also assigned to peak C.

(2) PSII Core and LHCP Fractions. In order to simplify both the DSC trace and the gels, by eliminating the dominant contribution of the multiple LHCP, we have separated the PSII core proteins from the LHCP and examined the DSC and thermal gel analysis behavior of both fractions. The expected protein compositions of these two fractions are given in Table I. Because we optimized the separation procedure for the purity of the PSII core fraction, our LHCP fraction is contaminated by some of the PSII core proteins. In contrast to the results of Ghanotakis and Yocum (1986), our PSII core preparations retain a significant fraction of the 17- and 23-kDa proteins. However, these PSII core samples exhibit only 47% activity in the absence of added calcium, which indicates that the 17- and 23-kDa polypeptides are not functionally bound to all PSII centers. This PSII core isolation procedure is also known to perturb the electron acceptor side properties of PSII (Ghanotakis & Yocum, 1986). Therefore, both the electron donor and electron acceptor side of the electron-transport chain are heterogeneous in the PSII core preparation.

The separation of PSII into the PSII core and the LHCP fractions can aid in assigning the DSC peaks, if the peaks in the DSC traces of the fractions are comparable to the peaks of the original PSII complex. Figure 2 compares the DSC behavior of the PSII core and the LHCP fractions with that of PSII membranes under the same conditions (pH 7.5, 0.01% TX-100). In the high-temperature range (peaks C and D), the sum of the DSC traces of the two component fractions (Figure 2b,c) is comparable to that of PSII membranes (Figure 2a). The comparison suggests that peak D, the dominant peak in the DSC trace of the LHCP fraction, is the denaturation of the LHCP and peaks A–C are the denaturation of the PSII core proteins. The small peak C in the DSC scan of the LHCP

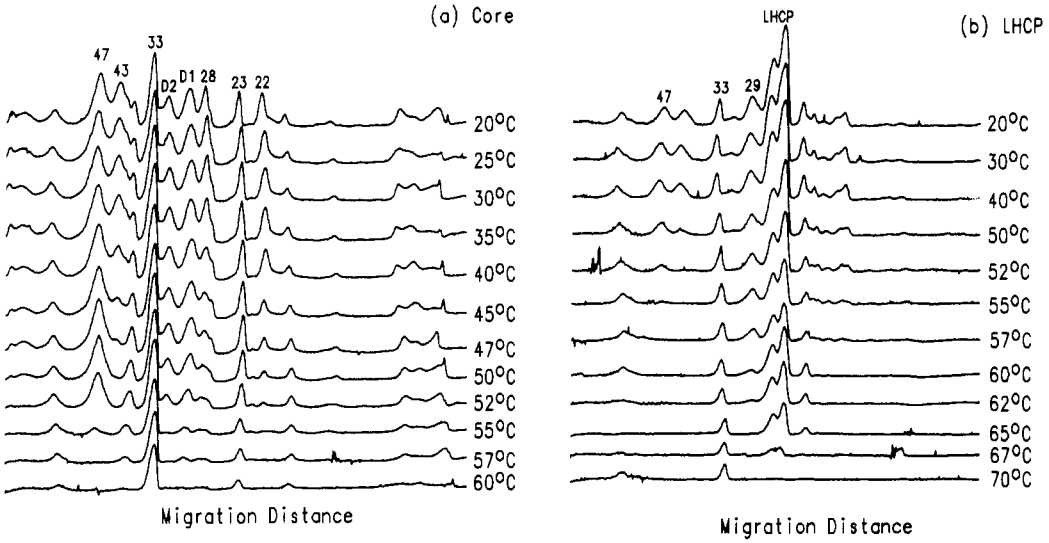

FIGURE 3: SDS–PAGE of heated aliquots of PSII core and LHCP preparations for the determination of protein denaturation temperatures by thermal gel analysis. The peaks in the densitometer scans of (a) PSII core and (b) LHCP preparations which correspond to PSII proteins studied in this thermal gel analysis experiment are labeled by name or approximate molecular mass (kDa). Each scan is labeled with the temperature to which the aliquot was heated.

fraction is probably due to contamination of the LHCP fraction by PSII core proteins (see gels in Figure 3). The low-temperature region of the DSC trace, which consists of peaks A_2 and B, is not equivalent in the PSII core and the PSII membrane samples. The broad 33–38 °C component in the DSC trace of the PSII core fraction (Figure 2c) is likely to correspond to peak A_2, since the heat inactivation of O_2 evolution activity occurs over the 30–40 °C range, and the broad 45–47 °C peak is likely to correspond to peak B. The broadness of peaks A_2 and B is probably due to the heterogeneity both of extrinsic polypeptide binding, which has been shown to alter peak A_2 (Thompson et al., 1986), and of the electron acceptor side, which is likely to be damaged during peak B (discussed below). Thus, the DSC behavior of the PSII core and LHCP samples is roughly consistent with our prior DSC studies of PSII membranes. However, the heterogeneity of the A_2 and B peaks in the PSII core preparation suggests that, despite the removal of the dominant LHCP fraction of the sample, the low-temperature DSC peaks are best studied in a more homogeneous PSII membrane sample.

On the other hand, removal of the LHCP allows us to use thermal gel analysis to determine the denaturation temperatures of several proteins which are not well resolved by gel electrophoresis of PSII membrane samples, in particular, the 28- and 29-kDa proteins and the important D1 and D2 proteins. Because of this advantage, and the opportunity to confirm independently the results of the thermal gel analysis studies of PSII membranes, we used thermal gel analysis to assign the DSC peaks of both the PSII core and LHCP fractions to the denaturations of the protein components. Figure 3 shows the gel electrophoresis separation of the proteins of both fractions in aliquots heated to different temperatures, to illustrate the thermal gel analysis method and to demonstrate the separation of the LHCP and PSII core proteins. In the PSII core fraction (Figure 4a), we observe no proteins denaturing during the broad A_2 peak, three proteins denaturing during the broad (45–47 °C) B peak (43 kDa at 43 °C, 28 kDa at 46 °C, and 22 kDa at 45 °C), and three proteins denaturing during the 53 °C C peak (47 kDa at 52 °C, D1 at 52 °C, and D2 at 51 °C). In the LHCP sample (Figure 4b), the small peak C (52.5 °C) is assigned to the denaturation of PSII core protein impurities, such as the 47-kDa protein (51 °C), and peak D (66 °C) is assigned to the

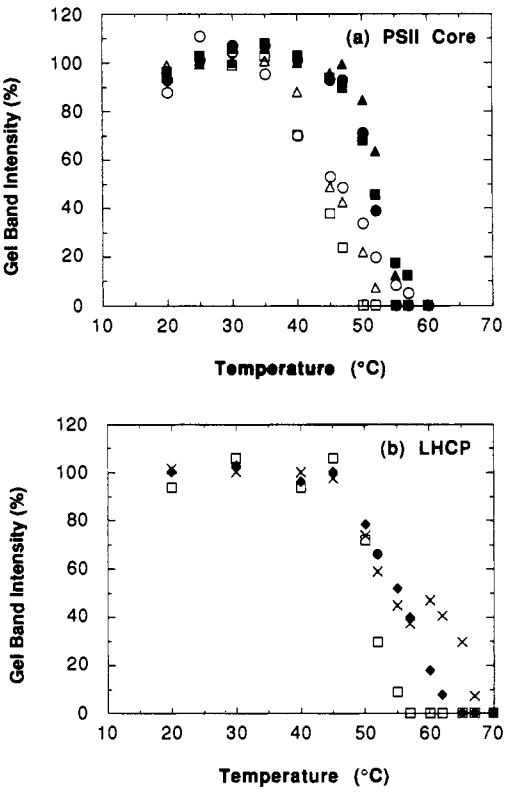

FIGURE 4: Thermal gel analysis of protein denaturation temperatures in PSII core and LHCP preparations. Gel band intensities (of peaks in gel lanes shown in Figure 3) are plotted as a function of the temperature to which the aliquot was heated. (a) PSII core fraction: the proteins represented by open symbols, 43 kDa (□, $T_{1/2}$ = 43 °C), 28 kDa (○, $T_{1/2}$ = 46 °C), and 22 kDa (△, $T_{1/2}$ = 45 °C), denature at approximately the temperature of peak B (45–47 °C); the proteins represented by closed symbols, D1 (■, $T_{1/2}$ = 52 °C), D2 (●, $T_{1/2}$ = 51 °C), and 47 kDa (▲, $T_{1/2}$ = 52 °C), denature at approximately the temperature of peak C (53 °C). (b) LHCP fraction: the LHCP (×, $T_{1/2}$ = 56, 57 °C) and the 29-kDa protein (♦, $T_{1/2}$ = 55 °C) are assigned to peak D, and the 47-kDa protein (□, $T_{1/2}$ = 51 °C) is assigned to peak C, as described in the text.

denaturation of both of the LHCP (56 and 57 °C) and the 29-kDa protein (55 °C). In both PSII membranes and the LHCP fraction, the LHCP and 29-kDa proteins denature at temperatures below that of peak D (see Table II). This is most

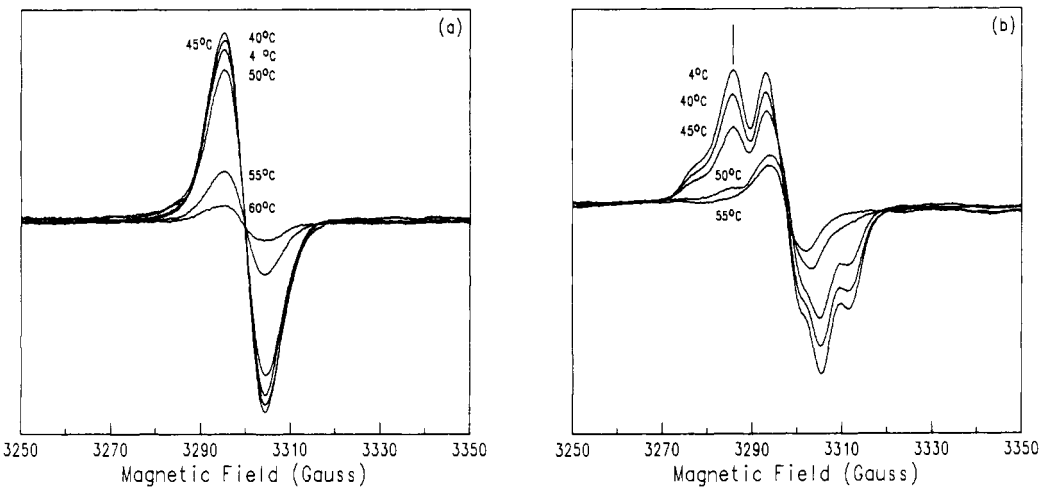

FIGURE 5: Heat inactivation of low-temperature Chl photooxidation and the dark-stable Tyr_D+. (a) 77 K illuminated-minus-dark spectra of the Chl cation radical produced in samples heated to the indicated temperatures. (b) Dark spectra of Tyr_D+ present in samples heated to the indicated temperatures. The line indicates the peak measured for the determination of the amount of Tyr_D+. EPR spectrometer conditions: microwave frequency, 9.1 GHz; microwave power, 0.4 mW; field modulation frequency, 100 kHz; field modulation amplitude, 4 G; sample temperature, 70 K.

likely due to overlap between the gel bands of the 29-kDa and D1 proteins, and between the LHCP and 28-kDa proteins. The correlations between DSC peak temperatures and protein denaturation temperatures in the PSII core and LHCP fractions are largely consistent with the results with intact PSII samples, as shown in Table II.

Heat Inactivation Temperatures. These assignments of the DSC peaks to the denaturations of individual proteins in the PSII complex complement our earlier assignments of peaks A_2 and B to the denaturations of O_2 evolution and electron-transport activity, respectively. In order to investigate the basis of the loss of DPC → DCIP electron-transport activity during peak B, we have studied the heat denaturation of a simpler function, utilizing EPR spectroscopy. The low-temperature photooxidation of Chl, which results in the $Chl^+Q_A^-$ charge separation, occurs when electron donation from water is blocked (for instance at 77 K) and cytochrome b_{559} is chemically oxidized (de Paula et al., 1985). In order to determine the temperature of denaturation of this activity, aliquots of a PSII sample (under conditions equivalent to that of the DSC sample) were heated to various temperatures and then treated with 2.5 mM $K_3Fe(CN)_6$ to oxidize cytochrome b_{559}. The EPR light-minus-dark difference spectra of the Chl cation radical in the heated samples are shown in Figure 5a. Figure 6 shows that the denaturation of the photooxidation of Chl ($T_{1/2}$ = 53 °C) correlates with the denaturation of DPC → DCIP electron transport ($T_{1/2}$ = 52 °C). Thus, both of these activities denature during peak B (53 °C under these conditions, data not shown).

We also observed that the EPR signal from the dark-stable radical, Tyr_D+, decreased in intensity upon heating (Figure 5b). As shown in Figure 6, this decrease ($T_{1/2}$ = 45 °C) correlates with the temperature of loss of water oxidation activity ($T_{1/2}$ = 46 °C). We conclude that Tyr_D+ undergoes a decrease in stability during the A_2 peak (47.5 °C under these conditions, data not shown). A decrease in the stability of this species has been observed to occur upon the removal of the three extrinsic proteins and Mn (Lozier & Butler, 1973).

DSC Investigations of the A_2 Peak. The correlation of heat inactivation and protein denaturation with the DSC peaks has resulted in several puzzling questions regarding the denaturation of the water-oxidizing apparatus. This denaturation occurs during the abnormally sharp A_2 peak (Thompson et al., 1986), which, as shown above, does not appear to correspond to the denaturation of any of the membrane proteins of PSII. We sought to understand the basis of the unusual sharpness of this peak with investigations of the effects of treatments on the DSC behavior. The A_2 peak is broadened by the removal of the 17- and 23-kDa extrinsic polypeptides or the presence of 1 mM ferricyanide, treatments which oxidize cytochrome b_{559}. Thus, the oxidation state of cytochrome b_{559} appears to influence the unusual cooperativity of the denaturation of the O_2-evolving apparatus (Thompson et al., 1986).

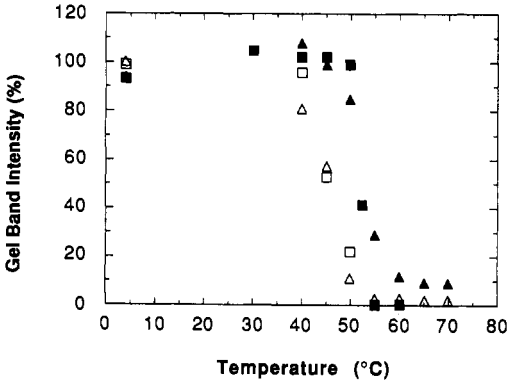

FIGURE 6: Correlation of the heat effect on activities observed by EPR with heat inactivation of electron transport. EPR signal intensities and electron-transport activities are plotted as a function of the temperature to which the sample was heated before the EPR or activity assay. Inactivation of Chl photooxidation (▲, $T_{1/2}$ = 53 °C) and DPC → DCIP electron transport (■, $T_{1/2}$ = 52 °C) correlate with DSC peak B (T_m = 53 °C). The decrease in the stability of Tyr_D+ (△, $T_{1/2}$ = 45 °C) and inactivation of H_2O → DCIP electron transport (□, $T_{1/2}$ = 46 °C) correlate with DSC peak A_2 (T_m = 47.5 °C).

Because chloride is an essential cofactor for O_2 evolution (Kelley & Izawa, 1978), we investigated the effects of the removal of Cl^- on the DSC denaturation profile. After Cl^- depletion, peak A_2 is broadened and shifted to lower temperature, and the other DSC peaks are not changed significantly, as shown in Figure 7. This effect is reversed by re-addition of Cl^- (Figure 7d). This result is consistent with a report that Cl^- depletion lowers the temperature of heat inactivation (Nash et al., 1985). Thompson et al. (1986) have also shown that peak A_2 occurs at lower temperatures at pH 7.5 (43 °C) than at pH 6.0 (48 °C), consistent with some evidence that OH^- binds competitively with Cl^- (Critchley, 1983; Homann, 1985). Thus, conditions which favor the

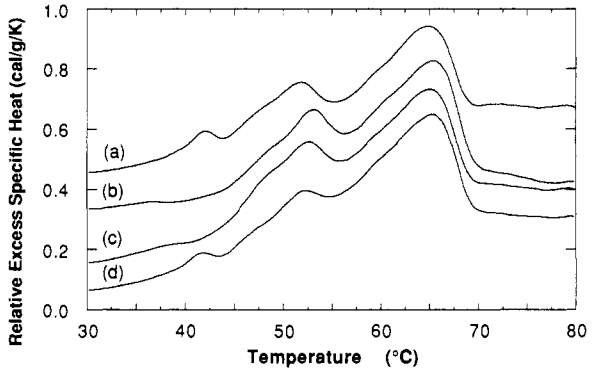

FIGURE 7: Effect of chloride depletion and reconstitution on peak A_2 in DSC scans of PSII membranes. DSC scans of (a) PSII in pH 7.5 buffer, (b) Cl^--depleted PSII, (c) Cl^--depleted PSII plus 0.1 mM NaCl, and (d) Cl^--depleted PSII plus 25 mM NaCl (equivalent $[Cl^-]$ as in sample a). Cl^--depleted samples were in Cl^- depletion buffer; all samples contain 0.01% TX-100.

binding of OH^- to the Cl^- binding site lower the temperature of the A_2 peak.

Another molecule known to bind to the Cl^- binding site is NH_2OH, which can reduce and release Mn, thus inactivating O_2 evolution (Beck & Brudvig, 1988). H_2O_2 is thought to react similarly with the Mn complex (Velthuys & Kok, 1978; Beck, 1988) and might be generated within the PSII sample by uncontrolled reactions of the water-oxidizing apparatus with water or OH^- at elevated temperatures. In order to test for the possible involvement of peroxide and superoxide in the release of Mn during peak A_2, we investigated the effects of catalase and superoxide dismutase on the DSC peaks. Both of these enzymes are sufficiently thermally stable to remain active at the temperatures of peak A_2 [T_m = 66 °C for catalase (Sochava et al., 1985), and superoxide dismutase loses only 5% of its activity in a 20-min incubation at 52 °C (Bucker & Martin, 1981)]. Including either of these enzymes in the PSII sample caused the A_2 peak to shift to higher temperature and broaden, with little effect on the remainder of the DSC trace, as shown in Figure 8. The spikes in the DSC scans which occur in the 50–70 °C range (in peak C of scan A and peak D of scan C) are thought to be due to clumping and settling of the PSII membrane suspensions in the pillbox cells of the Microcal-2 during the slow DSC scan. Such behavior was never observed in DSC scans of PSII membrane samples in the DASM-4, which has a helical cell geometry [see Figures 2 and 7 and Thompson et al. (1986)]. A similar problem has been observed for aspartate transcarbamoylase (Edge et al., 1988): the spikes were observed with these samples only in a calorimeter with pillbox-shaped cells. We conclude that the effects of catalase and superoxide dismutase on peak A_2 suggest that peroxide and superoxide are involved in the denaturation of O_2 evolution, perhaps in a reaction which results in the reduction and subsequent release of two Mn.

Discussion

The results of the assignments of the DSC peaks to the denaturations of the individual proteins of the PSII complex are summarized in Table II. In each case, the proteins denaturing during one DSC peak may denature as one cooperative unit, which suggests that PSII is composed of the following structural units: (1) a core unit consisting of D1, D2, cytochrome b_{559}, the 47-kDa protein, and the 10-kDa protein; (2) a unit consisting of the 43-, 28-, and 22-kDa proteins; and (3) an antenna unit consisting of the two LHCP and the 29-kDa protein. Although it is always possible that a protein could exhibit an apparent change in solubility which is not due

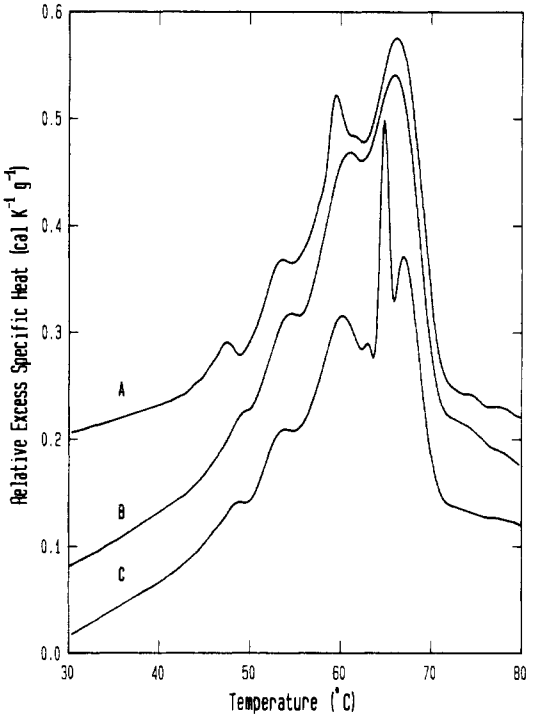

FIGURE 8: Effect of catalase and superoxide dismutase on DSC scans of PSII membranes. DSC scans of (A) PSII alone, (B) PSII plus 30 μg/L superoxide dismutase, and (C) PSII plus 60 μg/L catalase, all in pH 6.0 buffer with 0.01% TX-100.

to its denaturation, or that two distant proteins could denature at the same temperature by coincidence, the structural organization suggested by the assignments of the DSC peaks is consistent with the results of biochemical separations of PSII membrane samples into smaller complexes. The PSII core preparation procedure used in this work separates the two LHCP and the 29-kDa proteins from the remainder of the PSII proteins, consistent with the denaturation of these three proteins as a separate unit in peak D. The further purification of the PSII core preparation by fast-performance liquid chromatography removes the 28-, 22-, and 10-kDa proteins (Ghanotakis et al., 1987a). This is consistent with the observation that the 28- and 22-kDa proteins denature in a separate cooperative unit in peak B. It has also been shown that the 43-kDa protein can be removed from a chlorophyll/protein complex, leaving a complex which consists of the 47-kDa protein, D1, D2, and cytochrome b_{559} (Yamagishi & Katoh, 1984; Akabori et al., 1988). Finally, the recent isolation of a complex containing only D1, D2, and cytochrome b_{559} is consistent with the denaturation of these proteins within one cooperative unit during peak C. This structural information also contributes to our understanding of the functions of the individual proteins, because closely associated proteins may cooperate to perform a common function. For instance, the degree of association of a Chl binding protein with the proteins which function in electron transport may indicate whether that protein functions solely in light harvesting (such as the 29-kDa protein) or has an additional role (such as the closely associated 47-kDa protein). Thus, the results of thermal gel analysis combined with DSC provide new insight into the structural organization of the multicomponent PSII complex, as well as the roles of the component proteins, by identifying possible structural and functional units within the native complex.

The correlation of DSC peaks with protein denaturations also yields a more detailed understanding of the denaturation of the PSII complex. We have shown that the lowest tem-

perature denaturation process, the denaturation of O_2 evolution activity during peak A_2, does not correlate with the denaturation of any of the major membrane proteins of PSII. We have not attempted to determine the denaturation temperature of the extrinsic proteins: the thermal gel analysis results for these proteins do not show a sharp denaturation (see 33- and 23-kDa bands in Figure 3a), which is not surprising because these extrinsic proteins may not undergo a substantial decrease in solubility upon denaturation. In addition, heating may dissociate these proteins from the insoluble PSII complex which could *increase* their solubility. Thus, the possibility that these extrinsic proteins dissociate or denature during the A_2 peak is not ruled out by our experiments. However, Nash et al. (1985) have shown that loss of O_2 evolution activity precedes dissociation of these proteins. The following summarizes the probable sequence of events which occurs during the A_2 peak: (1) two Mn are released (Cramer et al., 1981; Nash et al., 1985), which results in the loss of O_2 evolution activity (Thompson et al., 1986); (2) the change in structure upon release of Mn may lead to the dissociation of the extrinsic proteins, which in turn causes the observed decrease in the reduction potential of cytochrome b_{559} (Cramer et al., 1981) and the decrease in the stability of Tyr_{D^+}. The effects of several treatments on the A_2 peak have led us to propose a mechanism for the reaction which results in the release of Mn, which will be discussed below.

The denaturation of the 43-, 28-, and 22-kDa proteins which occurs during peak B results in the loss of DPC → DCIP electron transport and low-temperature Chl photooxidation. This is unexpected, because almost all of the electron-transport chain components required for these two activities are likely to be on the D1 and D2 proteins, which do not denature until peak C. One explanation for the loss of both of these activities is that the denaturation of the 22- or 28-kDa protein may perturb the primary quinone electron acceptor, Q_A. The removal of the 22- or 28-kDa protein from a PSII core preparation probably perturbs quinone binding at the Q_B site, since preparations lacking these proteins exhibit greater O_2 evolution activity with ferricyanide than with quinone electron acceptors, and this activity is insensitive to DCMU, an inhibitor which binds to the Q_B site (Ghanotakis et al., 1987b). We suggest that it is the denaturation of the 22- or 28-kDa protein which perturbs Q_A and causes the loss of electron transport and Chl photooxidation which occurs during peak B.

In the absence of the correlation between protein denaturations and DSC peaks, Thompson et al. (1986) suggested that peaks C and D corresponded to the denaturation of the LHCP, because of their large area and the effect of Mg^{2+} on peak C. We now confirm that peak D is the denaturation of the LHCP but peak C is the denaturation of the PSII reaction center. The 29-kDa Chl protein also denatures during peak D, suggesting that it is also a peripheral antenna protein. The Chl proteins which denature during peaks B and C (47, 43, and 28 kDa) are known to bind only Chl *a*, and therefore thought to be more closely associated with the reaction center (Green, 1988; Ghanotakis et al., 1987a), consistent with their denaturation in these DSC peaks. The denaturation of the 47-kDa and 10-kDa proteins during peak C suggests that these proteins are closely associated with the D1/D2/cytochrome b_{559} PSII reaction center. The effects of Mg^{2+} and detergent on peaks C and D (Thompson et al., 1986) can now be reinterpreted in light of the identification of the proteins denaturing during these DSC peaks. In the absence of Mg^{2+}, peaks C and D merge, which may indicate a tighter association between the PSII core and the LHCP into a single cooperative unit. This is consistent with the observed decrease in energy transfer between PSII complexes under Mg^{2+}-deficient conditions (Melis & Homann, 1978). An increase in the detergent concentration (in a range with no irreversible effects on activity) broadens peak D more than any of the other DSC peaks. Most likely, the higher detergent concentrations separate the LHCP from the PSII core and from each other such that the cooperativity of their denaturation is decreased and peak D is broadened.

The assignment of the DSC denaturation profile of the PSII membrane protein complex using heat inactivation and thermal gel analysis studies has thus provided insight into the structure of PSII, the roles of the component proteins, and the steps, at the level of proteins and associated cofactors, in the thermal denaturation process. Such an approach may prove useful in the study of other large membrane protein complexes.

We also sought a more detailed picture of the denaturation of the heat-sensitive O_2-evolving apparatus and have developed a model for the mechanism of this denaturation which accounts for the effects of treatments on the temperature and shape of the DSC peak A_2. Release of Mn, which is likely to occur during peak A_2, is known to be induced by a number of treatments of PSII samples (heat, detergent, Tris, NH_2OH). The reaction with NH_2OH has been relatively well-studied and is thought to occur via reduction of the Mn (Beck & Brudvig, 1987). The Mn complex is likely to consist of four Mn(III) in the dark-stable S_1 state (Ananyev et al., 1988). Reduction of the Mn complex should eventually cause the release of Mn, because of the decreased ligand field stabilization of Mn(II) complexes (Cotton & Wilkinson, 1980). Both NH_2OH (Bouge, 1971) and H_2O_2 (Velthuys & Kok, 1978) are known to cause a two-flash delay in the flash-dependent O_2 evolution pattern, which has been shown to be due to a two-electron reduction of the Mn complex from the S_1 to the S_{-1} state (Beck & Brudvig, 1987). A further reduction of the Mn beyond the stable S_{-1} state has been proposed to be the cause of Mn release by NH_2OH (Beck & Brudvig, 1987). The observed increase in the temperature of peak A_2 in the presence of catalase suggests that the heat-induced release of Mn may involve a similar reduction of Mn by peroxide.

The generation of peroxide within the sample could occur if the Mn complex somehow oxidizes water in a dark reaction. It is likely that because the active-site Mn complex must be highly oxidizing in order to oxidize water, it must be kept sequestered from the water phase in order to avoid uncontrolled reactions with water. It has been observed that the water binding site on the Mn complex is not in fast exchange with bulk water (based on a water proton relaxation rate enhancement of less than 1%; Srinivasan & Sharp, 1986), consistent with low solvent accessibility to this site. The observation that decreasing the $[Cl^-]$ or increasing the $[OH^-]$ lowers the temperature of peak A_2 suggests that OH^- binding at the Cl^- site, which is thought to be near the Mn complex (Beck & Brudvig, 1988), accelerates the heat-induced release of Mn. Since OH^- is more easily oxidized than water, it seems likely that it is the oxidation of OH^- at the nearby Cl^- binding site which produces peroxide within the PSII sample. Therefore, we propose that upon heating, the solvent accessibility of the Mn complex increases until the Mn complex oxidizes OH^- to produce H_2O_2, which can further reduce the Mn such that two Mn are released:

$$2OH^- + S_1 \rightarrow H_2O_2 + S_{-1} \quad (1)$$

$$H_2O_2 + S_{-1} \rightarrow \text{“}S_{-3}\text{”} + O_2 + 2H^+ \quad (2)$$

$$\text{"}S_{-3}\text{"} \rightarrow 2Mn^{2+}_{free} + 2Mn^{2+}_{bound} \quad (3)$$

The involvement of superoxide could be explained by a reaction analogous to reaction 1 which produces superoxide, which could reduce the Mn complex in reactions analogous to eq 2 and 3.

The proposed reactions are supported by prior studies of the reduction and extraction of Mn by NH_2OH and H_2O_2. The S_1 state can be reduced to S_{-1} by H_2O_2 or by NH_2OH (Bouge, 1971; Velthuys & Kok, 1978). The S_1/S_{-1} reduction potential has been estimated to be $\approx$0.4 V (Velthuys & Kok, 1978), on the basis of this irreversible reaction with H_2O_2 (E_m = 0.27 V for O_2/H_2O_2). Since the $H_2O_2/2OH^-$ reduction potential is about 0.45 V (calculated from the H_2O_2/H_2O reduction potential), OH^- should be able to reduce S_1 to S_{-1}, as proposed in reaction 1. Reaction 2 can be justified by a consideration of the reactions of NH_2OH with the Mn complex. NH_2OH not only can reduce the Mn to the S_{-1} state but also can extract the Mn, presumably by a further reduction to the S_{-3} state (Beck & Brudvig, 1987). H_2O_2 has been suggested to react similarly (Beck, 1988) and has been reported to decrease the yields of O_2 evolution (Velthuys & Kok, 1978). Sandusky and Yocum (1988) have demonstrated that incubation of chloride-depleted PSII with H_2O_2 causes rapid Mn release and that Cl^- partially protects against this Mn release. Thus, it appears that the reduction of Mn in the S_1 and S_{-1} states by H_2O_2 is inhibited by Cl^-, suggesting that reactions 1 and 2 occur at the Cl^- binding site.

The release of Mn is expected when the four Mn are fully reduced to Mn(II). The proposed scheme presumes that the S_{-1} state consists of two Mn(III) and two Mn(II), which has been suggested on the basis of evidence that the assembly of the complex from Mn(II) to the first stable intermediate (S_{-1}) requires only two oxidations of Mn per PSII center (Ananyev et al., 1988). Then the "S_{-3}" state, produced by reaction 2, should consist of four Mn(II). The observed release of only two Mn in reaction 3 would occur if the Mn binding site can bind two Mn(II) sufficiently strongly to prevent their release, but upon reduction, the other two Mn are not stably bound. It has been reported that two of the four Mn are more tightly bound (Kuwabara & Murata, 1983), in agreement with the release of two Mn as suggested in reaction 3.

We propose that the unusual sharpness of the A_2 peak is due to a high activation energy barrier for reaction 1, because of the inaccessibility of the Mn site to the water phase. Although the penetrability of proteins by OH^- is not known quantitatively, it is expected to be low and to have a high activation energy (Englander & Kallenbach, 1984). The accessibility of the Mn site to OH^- should increase steeply with temperature, giving rise to a steep increase in the rate of the reaction. Thus, these reactions are not at equilibrium but are kinetically limited by a large activation energy, which explains the unreasonably large size of the cooperative unit obtained by a van't Hoff analysis of the A_2 peak (Thompson et al., 1986). Indeed, early studies of heat damage to photosynthesis reported a remarkably high activation energy barrier in the 51–95-kcal range (Rabinowitch, 1956). The expected behavior of a kinetically limited process, as discussed by Borchardt and Daniels (1951), is an asymmetric curve, broader on the low-temperature side. Perhaps then the broad underlying A_1 peak which was obtained in our earlier analysis of the DSC trace is actually not a distinct peak, but could instead be due to both a sloping base line and the broad, low-temperature side of the A_2 peak. Since both the presumed A_1 and the A_2 peaks correlate with the temperature of loss of O_2 evolution activity (Thompson et al., 1986), perhaps this denaturation actually occurs during a kinetically limited $A = A_1 + A_2$ peak.

It is difficult to estimate the enthalpy expected to correspond to the proposed reactions. The reduction potentials of the S states are not known, but reactions 1 and 2 are roughly equivalent to the reduction of four Mn(III) to four Mn(II), with the concomitant oxidation of two OH^- to O_2. However, we do not know the binding energy of the Mn complex, which must be overcome for reaction 3 to occur. A further reaction which may also be occurring during the A peak is the dissociation of the extrinsic polypeptides, which has been shown to follow the heat denaturation of O_2 evolution activity (Nash et al., 1985). Perhaps the change in structure upon release of the Mn decreases the affinity of the PSII complex for these polypeptides. Finally, it is possible that one or more of these extrinsic proteins denatures after its release from the complex, a denaturation which should have a more appreciable enthalpy and could account for the size of the A peak. It would be interesting to test this possibility by separating the extrinsic proteins from PSII samples heated to a range of temperatures and testing for their ability to rebind functionally to the PSII complex.

The proposed mechanism for the heat denaturation of the water-oxidizing apparatus can account for the observed effects of various treatments on the A peak. Removal of the extrinsic polypeptides or chloride and an increase in the pH from 6.0 to 7.5 all result in a decrease in the temperature of the A peak. This can be explained by an increase in the rate of reaction 1, caused by an increase in the accessibility of the Mn complex upon polypeptide removal or an increase in $[OH^-]$ at the chloride binding site. The oxidation of cytochrome b_{559} by 1 mM ferricyanide, which also results in a lower temperature A peak (Thompson et al., 1986), perhaps also causes an increase in the accessibility of the Mn site, due to a change in conformation or a resulting decrease in the affinity for the extrinsic polypeptides. The broadening of the A peak which occurs after some of these treatments can be explained if these treatments lower the activation barrier for reaction 1. The effect of catalase and superoxide dismutase on peak A is consistent with the fact that these enzymes would be expected to slow reaction 2 (or an analogous reaction involving superoxide) by scavenging one of the reactants. This would slow the overall denaturation occurring during peak A, which would result in a broader peak at higher temperatures as is observed. The A_2 peak is also more variable than the other DSC peaks, which we suggested to be due to variable degrees of loss of the 17- and 23-kDa polypeptides (Thompson et al., 1986). In view of the proposed model, another likely source of this variability is the range of aggregation of the PSII suspensions, which could alter the rate of reaction 1 by changing the accessibility of the Mn complex.

This model for the heat-induced denaturation of the water-oxidizing apparatus may also account for other instances of instability of the Mn complex. For instance, in the absence of the 33-kDa polypeptide, two Mn are released unless high concentrations of Cl^- (200 mM) are present (Miyao & Murata, 1984). This may be due to an increased accessibility of the Mn complex or a decreased Cl^- affinity both of which would increase the local $[OH^-]$ and promote reaction 1. The high $[Cl^-]$ could prevent the reduction of the Mn by OH^- by effectively excluding OH^- from the Cl^- binding site. We have noticed that intact PSII membranes also lose O_2 evolution activity more quickly after chloride depletion (L. Thompson, unpublished results). An alternate interpretation is that chloride stabilizes the binding of the 17- and 23-kDa extrinsic polypeptides (Homann, 1988) and the polypeptides may serve

to exclude OH^- from the vicinity of the Mn. However, this interpretation cannot explain the stabilizing effect of chloride in the absence of these polypeptides. Finally, the well-known difficulty in developing procedures to remove more of the PSII proteins from the complex without inactivating water oxidation may be due to the need to keep the Mn complex isolated from the bulk water phase throughout the isolation procedure. The procedure we chose for the isolation of the PSII core fraction, which retains particularly high O_2 evolution activity, maintains high $[Cl^-]$ (0.4 M NaCl) throughout the steps in which the sample is solubilized by the presence of high detergent concentrations (Ghanotakis et al., 1987a). Perhaps this high $[Cl^-]$ is needed, while the Mn complex is accessible to the water phase, to prevent it from oxidizing OH^-. The model we have described to explain the heat-induced release of Mn provides a new view of the requirements for stability of this complex. This may aid in the development of isolation procedures for simplified PSII reaction center preparations which retain O_2 evolution activity, and it may also explain the molecular basis of the unique heat sensitivity of the O_2-evolving apparatus in photosystem II.

References

Akabori, K., Tsukamoto, H., Tsukihara, J., Nagatsuka, T., Motokawa, O., & Toyoshima, Y. (1988) *Biochim. Biophys. Acta 932*, 345.

Ananyev, G. M., Shafiev, M. A., Isaenko, T. V., & Klimov, V. V. (1988) *Biofizika 33*, 265.

Babcock, G. T., Widger, W. R., Cramer, W. A., Oertling, W. A., & Metz, J. G. (1985) *Biochemistry 24*, 3638.

Beck, W. B. (1988) Ph.D. Thesis, Yale University.

Beck, W. F., & Brudvig, G. W. (1987) *Biochemistry 26*, 8285.

Beck, W. F., & Brudvig, G. W. (1988) *J. Am. Chem. Soc. 110*, 1517.

Beck, W. F., de Paula, J. C., & Brudvig, G. W. (1985) *Biochemistry 24*, 3035.

Berthold, D. A., Babcock, G. T., & Yocum, C. F. (1981) *FEBS Lett. 134*, 231.

Borchardt, H. J., & Daniels, F. (1951) *J. Am. Chem. Soc. 79*, 41.

Bouge, B. (1971) *Biochim. Biophys. Acta 234*, 103.

Brudvig, G. W., Beck, W. F., & de Paula, J. C. (1989) *Annu. Rev. Biophys. Biophys. Chem. 18*, 25.

Bucker, E. R., & Martin, S. E. (1981) *Appl. Environ. Microbiol. 41*, 449.

Chua, N.-H. (1980) *Methods Enzymol. 69*, 434.

Cotton, F. A., & Wilkinson, G. (1980) *Advanced Organic Chemistry*, p 739, Wiley, New York.

Cramer, W. A., Whitmarsh, J., & Low, P. S. (1981) *Biochemistry 20*, 157.

Critchley, C. (1983) *Biochim. Biophys. Acta 724*, 1.

Debus, R. J., Barry, B. A., Babcock, G. T., & McIntosh, L. (1988) *Proc. Natl. Acad. Sci. U.S.A. 84*, 427.

de Paula, J. C., Innes, J. B., & Brudvig, G. W. (1985) *Biochemistry 24*, 8114.

Edge, V., Allewell, N. M., & Sturtevant, J. M. (1988) *Biochemistry 27*, 8081.

Englander, S. W., & Kallenbach, N. R. (1984) *Q. Rev. Biophys. 16*, 521.

Ghanotakis, D. F., & Yocum, C. F. (1986) *FEBS Lett. 197*, 244.

Ghanotakis, D. F., Demetriou, D. M., & Yocum, C. F. (1987a) *Biochim. Biophys. Acta 891*, 15.

Ghanotakis, D. F., Waggoner, C. M., Bowlby, N. R., Demetriou, D. M., Babcock, G. T., & Yocum, C. F. (1987b) *Photosynth. Res. 14*, 191.

Green, B. R. (1988) *Photosynth. Res. 15*, 3.

Homann, P. H. (1985) *Biochim. Biophys. Acta 809*, 311.

Homann, P. H. (1988) *Plant Physiol. 88*, 194.

Ikeuchi, M., Yuasa, M., & Inoue, Y. (1985) *FEBS Lett. 185*, 316.

Katoh, S., & San Pietro, A. (1967) *Arch. Biochem. Biophys. 122*, 144.

Kelley, P. M., & Izawa, S. (1978) *Biochim. Biophys. Acta 502*, 198.

Kok, B., Forbush, B., & McGloin, M. (1970) *Photochem. Photobiol. 11*, 457.

Kuwabara, T., & Murata, N. (1983) *Plant Cell Physiol. 24*, 741.

Larsson, U. K., & Andersson, B. (1985) *Biochim. Biophys. Acta 809*, 396.

Lozier, R. H., & Butler, W. L. (1973) *Photochem. Photobiol. 17*, 133.

Michel, H., & Deisenhofer, J. (1988) *Biochemistry 27*, 1.

Miyao, M., & Murata, N. (1984) *FEBS Lett. 170*, 350.

Melis, A., & Homann, P. H. (1978) *Arch. Biochem. Biophys. 190*, 523.

Metz, J. G., Pakrasi, H. B., Seibert, M., & Arntzen, C. J. (1986) *FEBS Lett. 205*, 269.

Nanba, O., & Satoh, K. (1987) *Proc. Natl. Acad. Sci. U.S.A. 84*, 109.

Nash, D., Miyao, M., & Murata, N. (1985) *Biochim. Biophys. Acta 807*, 127.

Rabinowitch, E. I. (1956) *Photosynthesis and Related Processes II*, Part 2, p 1224, Interscience Publishers, New York.

Rigell, C. W., de Saussure, C., & Freire, E. (1985) *Biochemistry 24*, 5638.

Sandusky, P. O., & Yocum, C. F. (1988) *Biochim. Biophys. Acta 936*, 149.

Sochava, I. V., Belopolskaya, T. V., & Smirnova, O. I. (1985) *Biophys. Chem. 22*, 323.

Srinivisan, A. N., & Sharp, R. R. (1986) *Biochim. Biophys. Acta 850*, 211.

Tang, X.-S., & Satoh, K. (1985) *FEBS Lett. 179*, 60.

Thompson, L. K., Sturtevant, J. M., & Brudvig, G. W. (1986) *Biochemistry 25*, 6161.

Thompson, L. K., Sturtevant, J. M., & Brudvig, G. W. (1987) in *Progress in Photosynthesis Research* (Biggins, J., Ed.) Vol. I, p 609, Martinus Nijhoff Publishers, Dordrecht, The Netherlands.

Velthuys, B., & Kok, B. (1978) *Proc. Int. Congr. Photosynth., 4th, 1977*, 397.

Yamagishi, A., & Katoh, S. (1984) *Biochim. Biophys. Acta 765*, 118.

Zuber, H. (1985) *Photochem. Photobiol. 42*, 821.